American Journal of Pathology, Vol. 169, No. 1, July 2006

DOI: 10.2353/ajpath.2006.060085

Cell Injury, Repair, Aging and Apoptosis

Photoreceptor Cell Apoptosis in the Retinal Degeneration of *Uchl3*-Deficient Mice

Yae Sano,*† Akiko Furuta,* Rieko Setsuie,*† Hisae Kikuchi,* Yu-Lai Wang,* Mikako Sakurai,*† Jungkee Kwon,*‡ Mami Noda,† and Keiji Wada*

From the Department of Degenerative Neurological Diseases, National Institute of Neuroscience, National Center of Neurology and Psychiatry, Tokyo, Japan; the Laboratory of Pathophysiology,† Graduate School of Pharmaceutical Sciences, Kyushu University, Fukuoka, Japan; and the Laboratory of Animal Medicine,‡ College of Veterinary Medicine, Chonbuk National University, Jeonju, Korea*

UCH-L3 belongs to the ubiquitin C-terminal hydrolase family that deubiquitinates ubiquitin-protein conjugates in the ubiquitin-proteasome system. A murine *Uchl3* deletion mutant displays retinal degeneration, muscular degeneration, and mild growth retardation. To elucidate the function of UCH-L3, we investigated histopathological changes and expression of apoptosis- and oxidative stress-related proteins during retinal degeneration. In the normal retina, UCH-L3 was enriched in the photoreceptor inner segment that contains abundant mitochondria. Although the retina of *Uchl3*-deficient mice showed no significant morphological abnormalities during retinal development, prominent retinal degeneration became manifested after 3 weeks of age associated with photoreceptor cell apoptosis. Ultrastructurally, a decreased area of mitochondrial cristae and vacuolar changes were observed in the degenerated inner segment. Increased immunoreactivities for manganese superoxide dismutase, cytochrome *c* oxidase I, and apoptosis-inducing factor in the inner segment indicated mitochondrial oxidative stress. Expression of cytochrome c, caspase-1, and cleaved caspase-3 did not differ between wild-type and mutant mice; however, immunoreactivity for endonuclease G was found in the photoreceptor nuclei in the mutant retina. Hence, loss of UCH-L3 leads to mitochondrial oxidative stress-related photoreceptor cell apoptosis in a caspase-independent manner. Thus, *Uchl3*-deficient mice represent a model for adult-onset retinal degeneration associated with mitochondrial impairment. ***(Am J Pathol 2006, 169:132–141; DOI: 10.2353/ajpath.2006.060085)***

The ubiquitin system has been implicated in numerous cellular processes, including protein quality control, cell cycle, cell proliferation, signal transduction, membrane protein internalization, and apoptosis.[1,2] Ubiquitin-dependent processes are regulated by ubiquitinating enzymes, E1, E2, and E3, and deubiquitinating enzymes such as ubiquitin-specific proteases and ubiquitin C-terminal hydrolases (UCHs).[1,3–5] To date, four isozymes of UCHs, UCH-L1, UCH-L3, UCH-L4, and UCH-L5, have been cloned in mouse or human.[6–8] UCH-L1, also known as PGP 9.5, has been well characterized among the isozymes. UCH-L1 is selectively localized to brains and testis/ovaries[7] and functions as a ubiquitin ligase in addition to a deubiquitinating enzyme.[9] Furthermore, two distinct mutations are linked to Parkinson's disease in human[10] and gracile axonal dystrophy (*gad*) in mice.[11] UCH-L3, on the other hand, displays 52% amino acid identity to UCH-L1.[12] Uchl3 mRNA is expressed throughout various tissues and is especially enriched in testis and thymus.[13] In addition to its ubiquitin hydrolase activity, *in vitro* studies indicate that UCH-L3 cleaves the C terminus of the ubiquitin-like protein Nedd-8.[14,15] Although UCH-L1 and UCH-L3 are suggested to function as reciprocal modulators of germ cell apoptosis in experimental cryptorchid testis,[16] the cellular localization and function of UCH-L3 remain unknown in other organs.

Recently, *Uchl3*-deficient mice were generated with a deletion of exons 3 to 7, which are essential for hydrolase

Supported by grants-in-aid for scientific research from the Japan Society for the Promotion of Science; for priority area research from the Ministry of Education, Culture, Sports, Science and Technology, Japan; Kyushu University Foundation for Scientific Research from the Ministry of Health, Labour and Welfare, Japan; and the program for Promotion of Fundamental Studies in Health Sciences from the National Institute of Biomedical Innovation, Japan.

Accepted for publication March 23, 2006.

Address reprint requests to Akiko Furuta, M.D., Ph.D., Department of Degenerative Neurological Diseases, National Institute of Neuroscience, National Center of Neurology and Psychiatry, 4-1-1, Ogawahigashi, Kodaira, Tokyo 187-8502, Japan. E-mail: afuruta@ncnp.go.jp.

activity.[13] These mutant mice display postnatal retinal and muscular degenerations as well as mild growth retardation.[17] Retinal development is morphologically normal, but progressive retinal degeneration is reported to be evident at 3 months after birth.[17] However, precise chronological changes and the mechanism of the retinal degeneration in *Uchl3*-deficient mice has not been studied.

Both the caspase-dependent pathway and the caspase-independent pathway have been proposed to be involved in the models of retinal degeneration, including model animals for retinitis pigmentosa (such as Royal College of Surgeons (RCS) rat and retinal degeneration (*rd*) mice),[18] retinal detachment,[19] light injury,[20,21] ischemic injury,[22] and age-related macular degeneration.[23] In the ubiquitin system, UCH-L1 is involved in ischemia-induced apoptosis in the inner retina.[24] The role of UCH-L3 in retinal degeneration, however, is unclear.

To elucidate the function of UCH-L3, we investigated the histopathological changes and protein expression with respect to apoptotic pathways in *Uchl3*-deficient mice. Our results show that UCH-L3 is mainly localized to the photoreceptor inner segment that contains abundant mitochondria in the normal retina. *Uchl3*-deficient mice displayed caspase-independent apoptosis during postnatal retinal degeneration associated with increased expression of the markers for mitochondrial oxidative stress at the inner segment. We propose a possible antiapoptotic role of UCH-L3 in photoreceptor cells.

Materials and Methods

Animals

We used age-matched *Uchl3*-deficient mice and wild-type mice, all of which were offspring male from 15 to 20 pairs of heterozygotes that had been backcrossed with C57BL/6J at postnatal ages of 0 days (P0), 10 days (P10), 3 weeks (3w), 6 weeks (6w), 8 weeks (8w), and 12 weeks (12w). The total number of wild-type and *Uchl3*-deficient mice examined in the present study was 79, of which 30 mice were used for Western blotting, 42 mice were used for hematoxylin and eosin staining, immunohistochemistry, and terminal deoxynucleotidyl transferase-mediated dUTP nick end labeling (TUNEL) assay, and 7 mice were used for electron microscopy. The mice were maintained at the National Institute of Neuroscience, National Center of Neurology and Psychiatry (Tokyo, Japan). The experiments using the mice were approved by the Institute's Animal Investigation Committee.

Western Blotting

Eyes from P10-, 3w-, and 6w-old mice of both genotypes (10 mice in each time point, for a total of 30 mice) were lysed in protein lysis buffer (100 mmol/L Tris-HCl, pH 8.0, 300 mmol/L NaCl, 2% Triton X-100, 0.2% SDS, 2% sodium deoxycholate, 2 mmol/L EDTA) containing protease inhibitor (Complete protease inhibitor cocktail; Sigma-Aldrich, St. Louis, MO). The amount of total protein of each sample was determined by the Bio-Rad protein assay (Bio-Rad, Hercules, CA) using bovine serum albumin as a standard. Total protein (50 μg/lane) was separated by 15% SDS-polyacrylamide gels (Perfect NT Gel, DRC, Tokyo, Japan). Proteins were transferred to immuno-Blot polyvinylidene difluoride membranes (Bio-Rad) and incubated with 5% skim milk in TBST (50 mmol/L Tris-HCl-buffered saline, pH 7.0, containing 0.05% Triton X-100) for 1 hour at room temperature. The membranes were incubated with a 1:1000 dilution of each primary antibody for UCH-L1, UCH-L3,[25] and β-actin (1:1000; Sigma-Aldrich) overnight at 4°C. For the preparation of anti-mouse UCH-L1 antibody, histidine-tagged mouse UCH-L1 (6His-mUCH-L1) was prepared as described previously[26] and used to generate a polyclonal antiserum in rabbit (Takara, Tokushima, Japan). The polyclonal antibody was purified by affinity chromatography. The specificity of this antibody to the mouse UCH-L1 was verified by Western blotting using brain lysates from *gad* mice and wild-type mice (data not shown). The membranes were washed in TBST and further incubated with antimouse or rabbit IgG-horseradish peroxidase conjugate (1:1000; Chemicon, Temecula, CA). After washing in TBST, the membranes were developed with the Super Signal West Dura or Femto Extended Duration Substrate (Pierce, Rockford, IL) and analyzed with a ChemiImager (Alpha Innotech, San Leandro, CA). Western blotting was performed five times per each antibody.

Morphometric Analysis and Immunohistochemistry of Retina

Mice of both genotypes at P0, P10, 3w, 6w, 8w, and 12w of age (7 mice in each time point, total of 42 mice) were deeply anesthetized with diethylether, decapitated, and the eyes removed, immersion-fixed with 4% paraformaldehyde overnight at 4°C, and embedded in paraffin wax. Deparaffinized sections were stained with hematoxylin and eosin and examined under an Axioplan2 microscope (Carl Zeiss, Oberkochen, Germany) at a magnification $\times$400, and the thickness of each layer was measured using WinRoof software (Mitani Shoji, Tokyo, Japan).

For immunohistochemical studies, 5-μm-thick sagittal sections at the level of the optic nerve were deparaffinized and treated with 1% hydrogen peroxide (H_2O_2) for 30 minutes, incubated with 1% skim milk in phosphate-buffered saline (PBS, pH 7.4) for 1 hour at room temperature followed by incubation overnight at 4°C with each primary antibody for UCH-L1 and UCH-L3[25] diluted 1:500 in 1% skim milk in PBS. To characterize apoptosis- and oxidative stress-related proteins, antibodies to the following proteins were used; apoptosis-inducing factor (AIF; 1:500, Chemicon), caspase-1 (1:100; Cell Signaling Technology, Beverly, MA), caspase-3 (1:1000; Cell Signaling Technology), cleaved caspase-3 (1:50; Cell Signaling Technology), cytochrome *c* (1:1000; Santa Cruz Biotechnology, Santa Cruz, CA), cytochrome *c* oxidase I

(COX, 1:10,000; Molecular Probes, Eugene, OR), endonuclease G (Endo G; 1:500, Chemicon) and manganese superoxide dismutase (Mn-SOD; 1:10,000, Stressgen, Victoria, BC, Canada). The sections were washed in PBS and then incubated with biotinylated secondary antibodies diluted 1:500 in PBS containing 1% skim milk. The sections were treated with the VECTASTAIN Elite ABC kit (Vector Laboratories, Burlingame, CA) according to the manufacturer's protocol and developed with 0.02% 3,3′-diaminobenzidine tetrahydrochloride solution containing 0.003% H_2O_2. After visualization, sections were counterstained with hematoxylin. Sections were examined with an Axioplan2 microscope (Carl Zeiss). Immunohistochemistry was performed in at least three repeated experiments. The relative immunoreactivity for COX, Mn-SOD, AIF, and Endo G in each layer of mutant mice was compared with that of wild-type mice and was classified into no change (−), slight increase (±), mild increase (+), and marked increase (++).

TUNEL Staining

Apoptotic cells were examined in mice of both genotypes at P0, P10, 3w, 6w, 8w, and 12w (7 mice in each time point, for a total of 42 mice) by TUNEL stain using the Dead-End Fluorimetric TUNEL system kit (Promega, Madison, WI) according to the manufacturer's instructions. The sections were examined by using a confocal laser scanning microscope (Olympus, Tokyo, Japan). The microphotographs were captured at magnification ×400 (0.066 mm^2/each retinal section), positive cells were counted (Fluoview 2.0; Olympus), and the data were subjected to statistical analysis.

Electron Microscopic Analysis

3w-old mice of both genotypes (total 7 mice) were deeply anesthetized with 20% chloral hydrate aqueous solution and perfused with the following fixative: 2% paraformaldehyde, 2% glutaraldehyde in PBS, or sodium cacodylate buffer (pH 7.4). The eyes were removed and postfixed with the same fixative overnight at 4°C. The posterior segments of eyes were trimmed and washed with PBS or sodium cacodylate buffer, incubated in phosphate-buffered 1% osmium tetroxide for 1 hour, and dehydrated in ethanol and embedded in Epon 812 resin (TAAB, Berks, UK). Ultrathin sections (75 nm) were mounted on copper grids and stained with uranium acetate and lead citrate. The sections were observed using an H-7000 electron microscope (Hitachi, Tokyo, Japan). Morphometric analysis of mitochondria was performed by measuring average percentage of area occupied by cristae within a mitochondrion at the inner segment.

Statistical Analysis

In statistical analysis of thickness of retinal layers and TUNEL-positive cells, three wild-type and four *Uchl3*-deficient mice were used in each time point (P0, P10, 3w,

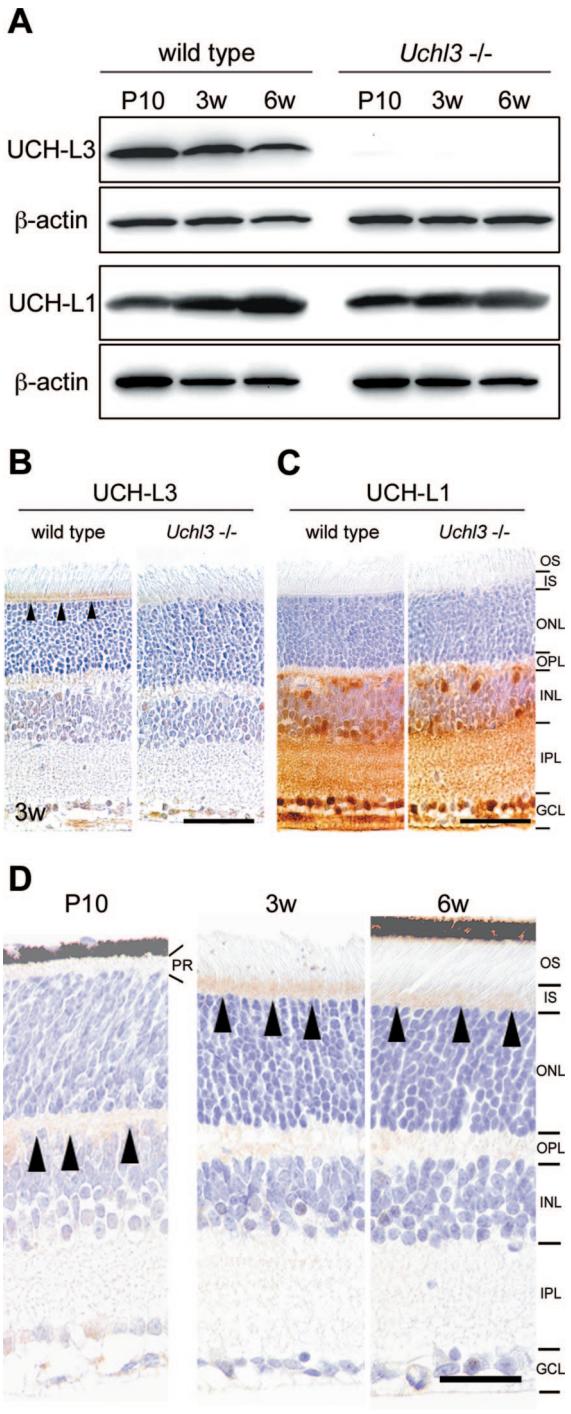

Figure 1. Expression of UCH-L1 and UCH-L3 in the retina of wild-type and *Uchl3*-deficient mice. **A:** Western blot analysis of UCH-L3 and UCH-L1 using whole-eye lysates from wild-type and *Uchl3*-deficient mice at P10, 3w, and 6w. The immunoreactive band for UCH-L3 is undetectable in *Uchl3*-deficient mice. Expression of UCH-L1 is similar between both genotypes. **B** and **C:** Immunohistochemistry for UCH-L3 (**B**) and UCH-L1 (**C**) in wild-type and *Uchl3*-deficient mice retinae at 3w. Immunoreactivity of UCH-L3 is found at the inner segment of the wild-type retina (**arrowheads**), whereas there is no significant immunoreactivity in *Uchl3*-deficient mice (**B**). UCH-L1 is expressed at the inner retina in both genotypes. **D:** Immunohistochemistry of UCH-L3 at P10, 3w, and 6w in wild-type retinae. UCH-L3 is faintly expressed in the outer plexiform layer at P10 (**arrowheads**). Thereafter, immunoreactivity for UCH-L3 is found in inner segment at 3w and 6w (**arrowheads**). PR, photoreceptor; OS, outer segment; IS, inner segment; ONL, outer nuclear layer; OPL, outer plexiform layer; INL, inner nuclear layer; IPL, inner plexiform layer; GCL, ganglion cell layer. Scale bars = 50 μm (**B** and **C**) and 20 μm (**D**).

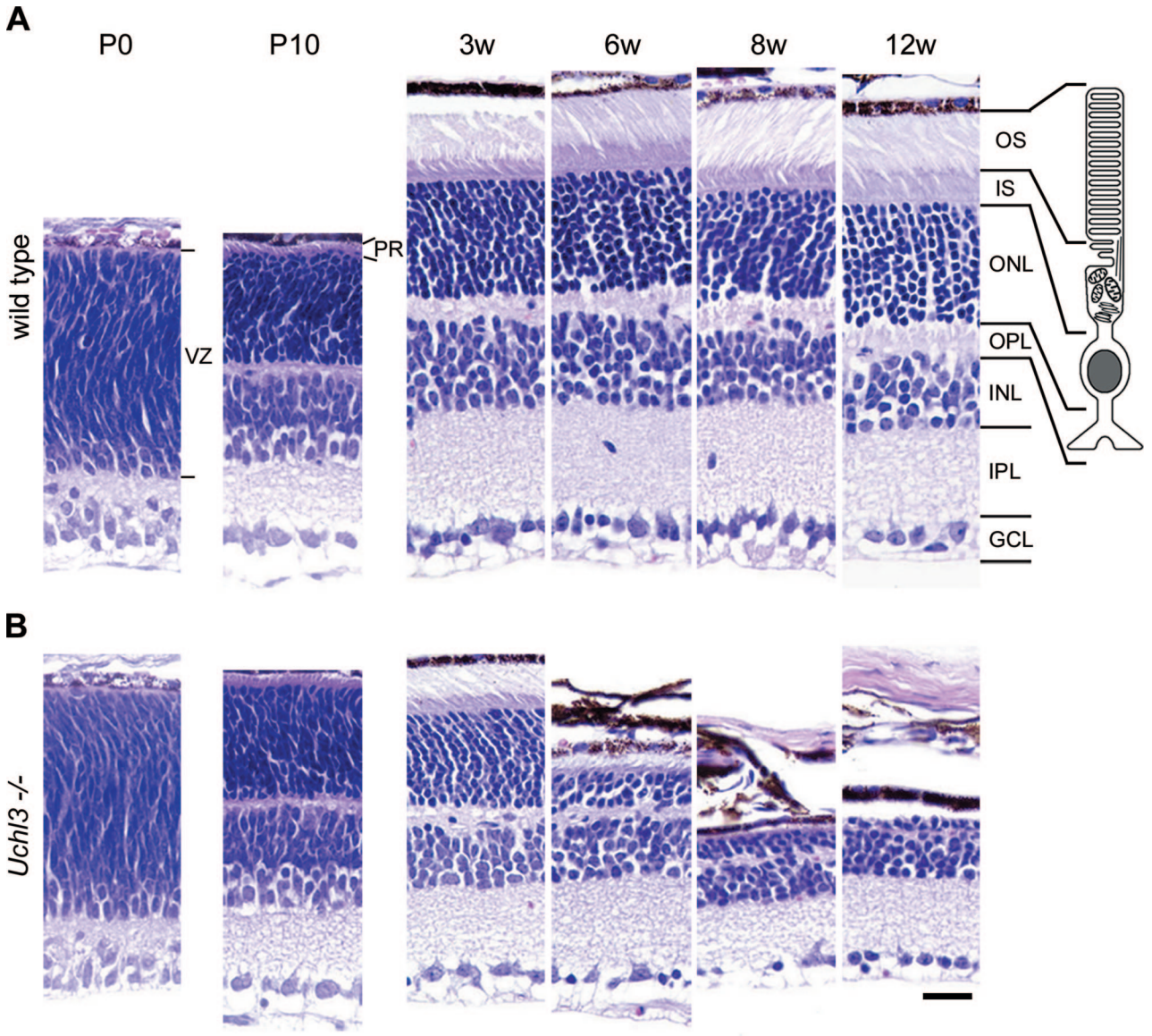

Figure 2. Histopathological changes of postnatal development in wild-type (**A**) and retinal degeneration of *Uchl3*-deficient mice (**B**) at P0, P10, 3w, 6w, 8w, and 12w. There is no morphological difference between both genotypes at P0 and P10, whereas outer and inner segments, outer nuclear layers, and outer plexiform layers are progressively degenerated after 3w of age. The illustration indicates a rod photoreceptor cell. VZ, ventricular zone; PR, photoreceptor; OS, outer segment; IS, inner segment; ONL, outer nuclear layer; OPL, outer plexiform layer; INL, inner nuclear layer; IPL, inner plexiform layer; GCL, ganglion cell layer. H&E staining. Scale bar = 20 μm (**A** and **B**).

6w, 8w, and 12w; for a total of 42 mice). The percentage of cristae area to whole mitochondrion in ultramicrophotographs was measured in 50 mitochondria of each genotype from three wild-type mice and four *Uchl3*-deficient mice, and the data were subjected to statistical analysis. All statistical analyses were carried out by Student's *t*-test using Microsoft Excel.

Results

Expression of UCH-L3 in the Murine Retina

Western blotting detected UCH-L3 (~30 kd) in extracts of eyes from wild-type mice at P10, 3w, and 6w, but the band was undetectable in *Uchl3*-deficient mice (Figure 1A). The expression level of UCH-L1 was similar in both genotypes. There was a tendency that the level of UCH-L3 decreased with age while the level of UCH-L1 increased with age in wild-type mice of all samples examined (five blots per antibody). Immunohistochemically, the cellular distribution of UCH-L3 differed from that of UCH-L1. UCH-L3 was enriched in the photoreceptor inner segment in wild-type mice at 3w of age (Figure 1B), whereas UCH-L1 was expressed in both genotypes in the inner retina, which consists of the inner nuclear layer, inner plexiform layer, and ganglion cell layer (Figure 1C). Localization of UCH-L3 in the wild-type retina was altered with age (Figure 1D). Immunoreactivity for UCH-L3 was not found at P0. UCH-L3 was faintly expressed in the outer plexiform layer at P10. Thereafter, it was localized to

inner segment at 3w. The inner segment was less immunoreactive for UCH-L3 at 6w, 8w, and 12w, compared with 3w.

Histopathological Changes of Retinal Degeneration in the Uchl3-Deficient Mice

Microscopic examination of retinal cross-sections revealed no obvious histopathological changes during early postnatal development at P0 and P10 in the retina of *Uchl3*-deficient mice (Figure 2). At 3w of age, the mutant retina began to degenerate in the inner segment and ultimately disappeared at 12w (Figures 2B and 3D). Thickness of the outer segment, outer nuclear layer, and outer plexiform layer was also significantly decreased in the mutant mice at 6w of age (Figure 3, C, E, and F). Despite the conspicuous change in the photoreceptor cells, the thickness of the mutant inner retina up to 12w of age was not altered compared with that of the wild-type (Figure 3, G–I).

Ultrastructurally, vacuolar changes were found in the inner segment of *Uchl3*-deficient mice at 3w of age (Figure 4). Mitochondria at the inner segment of mutant mice were slightly swollen. Groups of small round-to-oval structures were observed in the degenerated inner segment (Figure 4D), and these structures were considered to be the cross-sections of cell processes. Chromatin condensation in photoreceptor nuclei was sometimes seen in the outer nuclear layer at 3w (Figure 4F). Morphometric analysis showed that the percentage of cristae area to whole area of mitochondrion in the inner segment of *Uchl3*-deficient mice was significantly lower than that of wild-type mice (Figure 4, G and H).

Altered Expressions of Apoptosis-Related Proteins in the Degenerated Retina

Apoptotic cells in the retinal cross-sections were identified using the TUNEL staining. TUNEL-positive cells were identified in the ventricular zone at P0 and inner nuclear layer at P10 of both genotypes during the developmental period (Figure 5, A and C). The number of TUNEL-positive cells slightly increased in the inner nuclear layer at P10. After 3w of age, TUNEL-positive cells of mutant retina significantly increased at the outer nuclear layer of the mutant retina at 3w, 6w, and 8w (Figure 5, A and D).

To determine which apoptotic pathway was activated in *Uchl3*-deficient mice, we examined immunoreactivities of apoptosis-related proteins. Expression of cytochrome *c*, caspase-3, and cleaved caspase-3 and caspase-1, essential molecules for the caspase-dependent pathway, were unchanged in both genotypes (Figure 6A), whereas oxidative stress markers, COX and Mn-SOD as well as AIF and Endo G, indicators of the caspase-independent pathway, were altered in the mutant retina (Figure 6B). Chronological changes in expression of markers for oxidative stress and caspase-independent apoptosis at P0, P10, 3w, 6w, 8w, and 12w are shown in Table 1. The immunoreactivity of COX was increased in the inner segment at 3w and 6w. Mn-SOD was mildly increased in the inner segment at 3w, 6w, and 8w. Although AIF was enriched in the inner segment of *Uchl3*-deficient mice at 3w and 6w, nuclear labeling of AIF was not observed. On the other hand, Endo G was localized to the nuclei of the outer nuclear layer of the mutant retina at 3w and 6w. Expression of Endo G was slightly increased in the outer plexiform layer, inner nuclear layer, and inner plexiform layer of *Uchl3*-deficient mice after 3w of age (Table 1). Thus, degeneration of photoreceptor cells in *Uchl3*-defi-

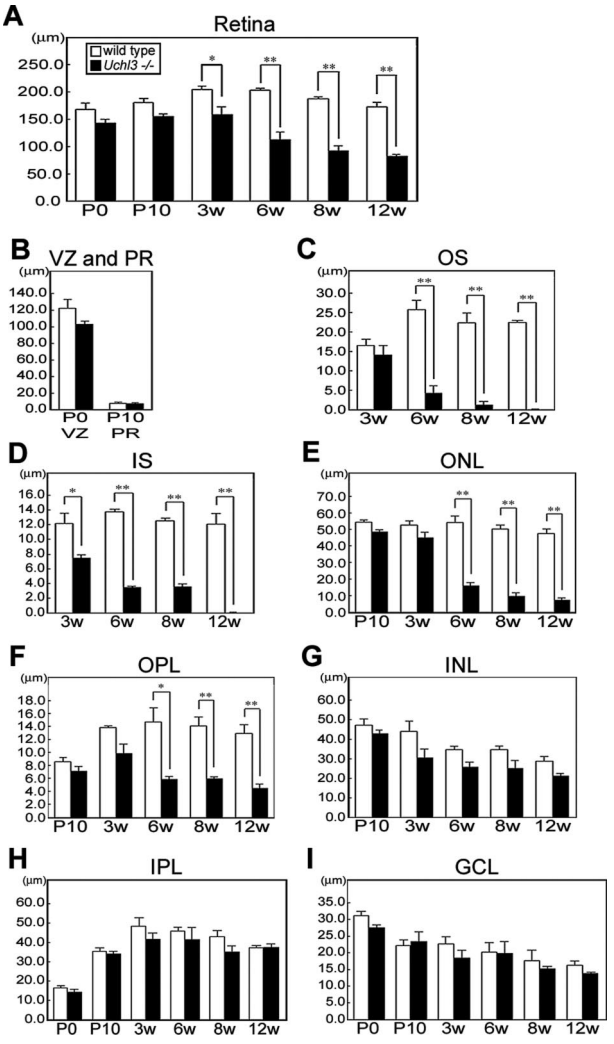

Figure 3. Chronological changes of retinal degeneration as assessed by thickness of each layer at different ages in wild-type and *Ucbl3*-deficient mice. **A:** Total retinal thickness is progressively decreased after 3w of age. **B:** Thickness of ventricular zone at P0 and photoreceptor layer at P10 shows no significant changes between both genotypes. **C–F:** Thickness of outer retinal layers in wild-type and *Ucbl3*-deficient mice at different ages. The earliest change is revealed at 3w of age in inner segment of mutant retina (**D**). Thickness of outer segment (**C**), outer nuclear layer (**E**), and outer plexiform layer (**F**) in *Ucbl3*-deficient mice is significantly decreased with age compared with that in the wild-type. **G–I:** Thickness of inner retinal layers in wild-type and *Ucbl3*-deficient mice at different ages. Thickness of inner nuclear layer (**G**), inner plexiform layer (**H**), and ganglion cell layer (**I**) are unchanged between both genotypes. Each value represents the mean ± SE ($*P < 0.05$; $**P < 0.01$). In all panels, the white bars represent the thickness in wild-type mice and the black bars represent the thickness in *Uchl3*-deficient mice. VZ, ventricular zone; PR, photoreceptor; OS, outer segment; IS, inner segment; ONL, outer nuclear layer; OPL, outer plexiform layer; INL, inner nuclear layer; IPL, inner plexiform layer; GCL, ganglion cell layer.

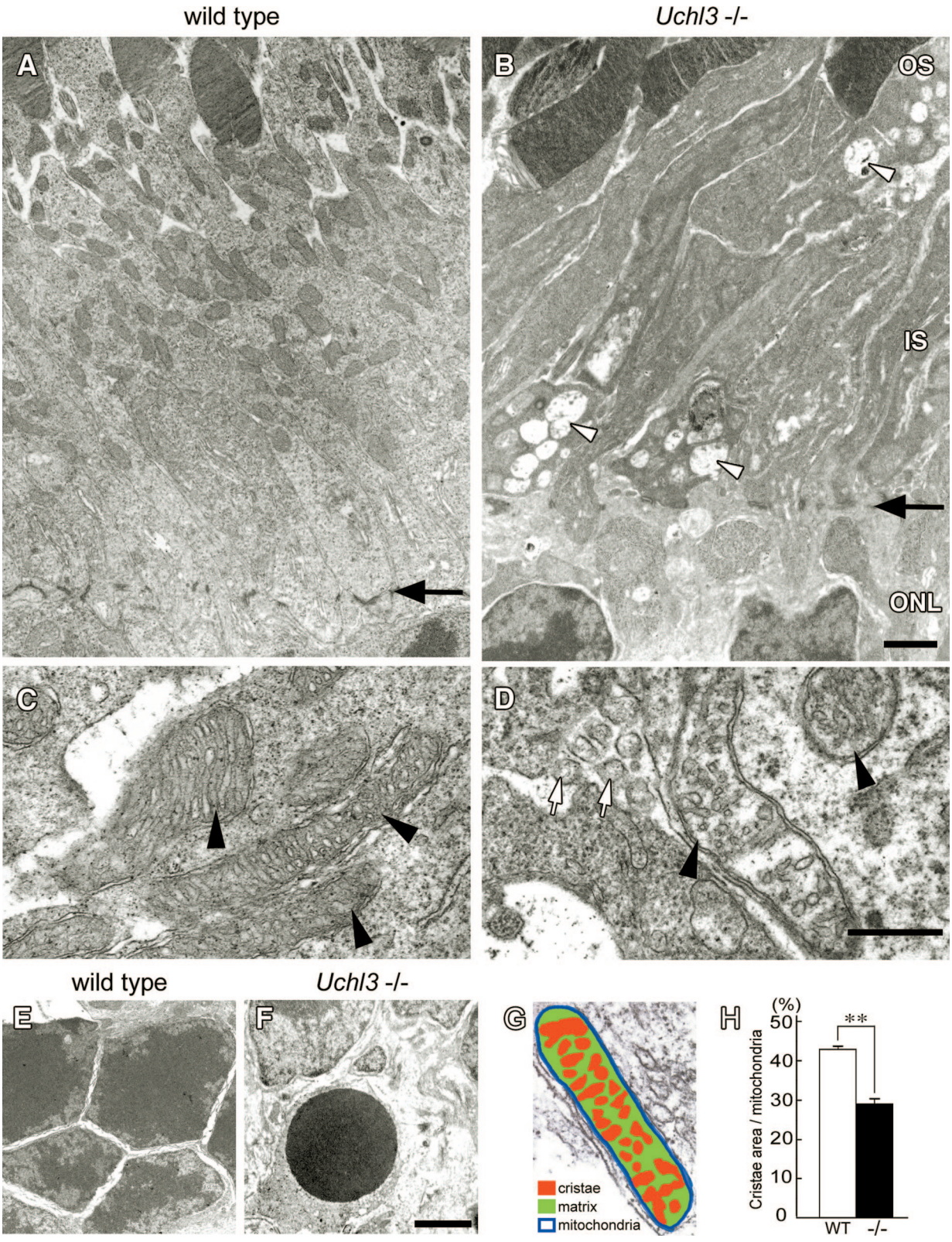

Figure 4. Ultrastructure of the outer retina in wild-type (**A**, **C**, and **E**) and *Uchl3*-deficient mice (**B**, **D**, and **F**) at 3w of age. **A** and **B:** Inner segment of mutant retina is shrunken associated with vacuolar changes (**arrowheads** in **B**). **Arrows** in **A** and **B** indicate outer limiting membrane. **C** and **D:** Subsets of mitochondria at the inner segment in *Uchl3*-deficient mice are swollen with decreased cristae (**arrowheads** in **D**) compared with that of wild-type (**arrowheads** in **C**). Groups of small round-to-oval shaped structures are occasionally seen in degenerated inner segment (**white arrows** in **D**). **E** and **F:** Outer nuclear layer of wild-type (**E**) and *Uchl3*-deficient (**F**) mice. Chromatin condensation of photoreceptor cells is observed in mutant mice (**F**)**. G** and **H:** Morphometric analysis of mitochondria was performed with the percentage of cristae area (**G**; **red**) against mitochondrial area ($n = 50$ for each genotype). Cristae area in the inner segment is significantly decreased in mutant retina (**H**, −/−, **black bar**) compared with that in wild-type (**H**, WT, **white bar**). Each value represents the mean ± SE (**$P < 0.01$). OS, outer segment; IS, inner segment; ONL, outer nuclear layer. Scale bars = 1 μm (**A** and **B**), 500 nm (**C** and **D**), and 1 μm (**E** and **F**).

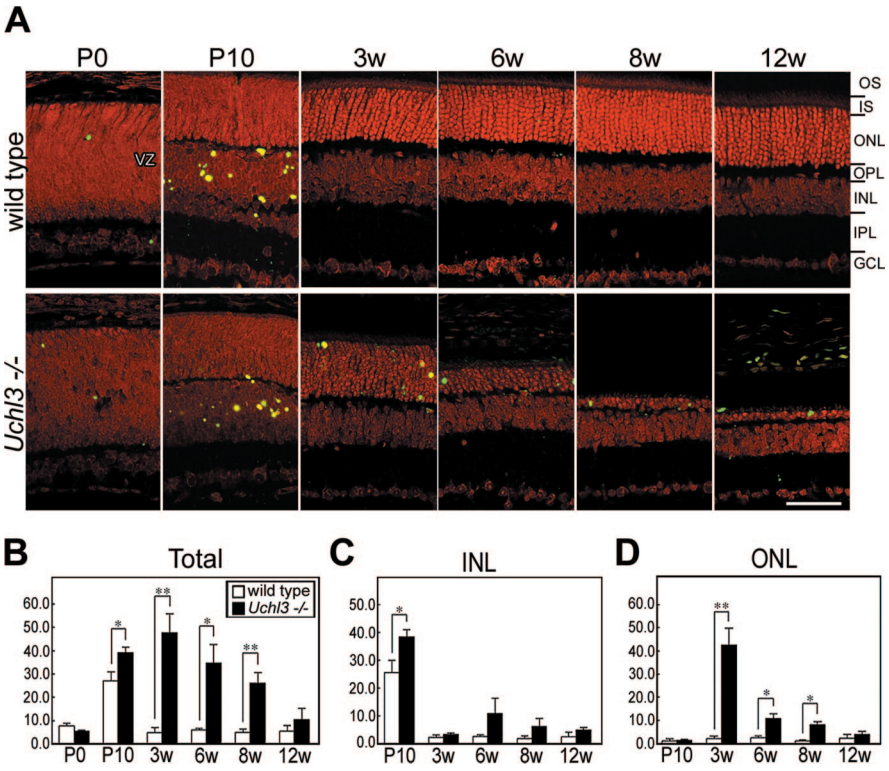

Figure 5. TUNEL analysis in wild-type and *Uchl3*-deficient mice at different ages. **A:** TUNEL staining in fluorescent microscopy shows that TUNEL-positive cells (**green**) are observed at the ventricular zone at P0 as well as at the inner nuclear layer at P10 in both genotypes. After 3w of age, TUNEL-positive cells are found in the outer nuclear layer in *Uchl3*-deficient mice. All sections are counterstained with propidium iodide (**red**). **B–D:** Number of TUNEL-positive cells in mutant mice (*Uchl3*$^{-/-}$; **black bar**) is significantly increased compared with those in wild-type (wild-type; **white bar**) at P10, 3w, 6w, and 8w (**B**). Increased number of TUNEL-positive cells in mutant mice at P10 correspond to apoptosis in the inner nuclear layer (**C**), whereas that in 3w, 6w, and 8w is reflected to apoptosis in the outer nuclear layer (**D**). VZ, ventricular zone; OS, outer segment; IS, inner segment; ONL, outer nuclear layer; OPL, outer plexiform layer; INL, inner nuclear layer; IPL, inner plexiform layer; GCL, ganglion cell layer. Scale bar = 20 μm (**A**). Each value in **B–D** represents the mean ± SE (*$P < 0.05$; **$P < 0.01$).

cient mice may be due to caspase-independent apoptotic pathway (Figure 7). Ubiquitin and Nedd-8, which are considered to be associated with UCH-L3 *in vitro*,[14,15] were expressed in the inner retina of both genotypes in a similar pattern as UCH-L1 (data not shown).

Discussion

This study demonstrates the unique localization of UCH-L3 to the photoreceptor inner segment that is abundantly populated with mitochondria after 3w of age in wild-type mice. The following features were found with regard to retinal degeneration in *Uchl3*-deficient mice. The retina showed no obvious morphological abnormalities during early postnatal development; however, progressive retinal degeneration was observed after 3w of age. The inner segment was originally perturbated with ultrastructural changes of mitochondria and increased expressions of markers for oxidative stress. The caspase-independent pathway was implicated during photoreceptor cell apoptosis. Thus, UCH-L3 may have a role in preventing mitochondrial oxidative stress-related apoptosis in photoreceptor cells.

Differential Localization of UCH-L1 and UCH-L3 in Murine Retina

The cellular distribution of UCH-L3 has not been studied except in the testis and epididymis, where UCH-L1 and UCH-L3 have distinct expression patterns.[25] In the present study, we found that UCH-L3 was enriched in the photoreceptor inner segment after 3w of age, whereas UCH-L1 was widely expressed in the inner retina. Photoreceptor cells are highly differentiated, and each segment has specific morphology and function; eg, inner segment contains abundant mitochondria,[27] and its oxygen consumption is considered to be high.[28] Meanwhile, expression of UCH-L1 at the inner retina was associated with that of ubiquitin and Nedd-8. Although *in vitro* studies indicate that UCH-L3 has de-neddylation activity,[14] UCH-L1 may be responsible for regulating expression level of ubiquitin and ubiquitin-like protein Nedd-8 in the retina. Because UCH-L1 expression in the retina was not altered in *Uchl3*-deficient mice, the function of UCH-L3 may not be compensated by UCH-L1. Our results indicate that UCH-L3 and UCH-L1 differ with regard to their localization and function in retina.

Mechanism of Photoreceptor Cell Death in the Uchl3-Deficient Mice

In our result, retinal apoptosis in *Uchl3*-deficient mice consisted of two different phases, during retinal development and after development. During the early postnatal development at P10, TUNEL-positive cells were observed in the inner nuclear layer of both genotypes, and the physiological apoptosis was slightly enhanced in the mutant retina. Because UCH-L3 was faintly expressed in the outer plexiform layer at P10 in wild-type mice, UCH-L3 may function during development. In the retinal development, the number of bipolar and Müller cell deaths reaches a peak at the postnatal days 8 to 11, which is associated with differentiation of the retina in

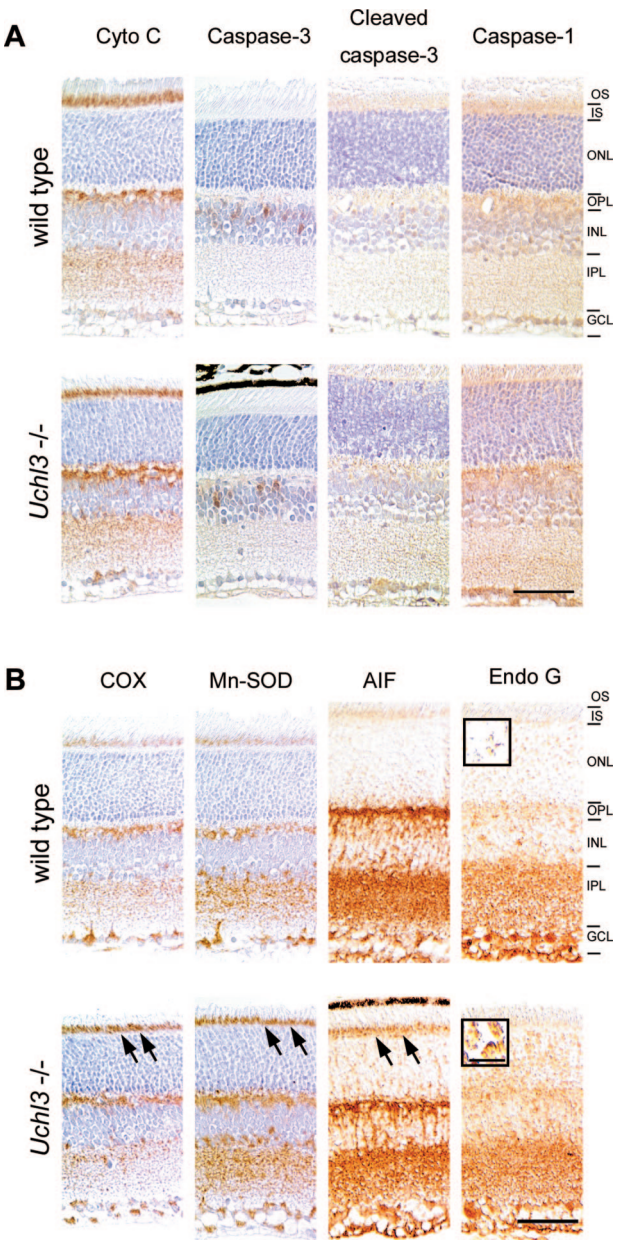

Figure 6. Immunohistochemical analysis of apoptosis- and oxidative stress-related molecules at 3w of age in wild-type and *Uchl3*-deficient mice. **A:** Expression of molecules relevant to the caspase-dependent pathway, including cytochrome *c* (Cyto C), caspase-3, cleaved caspase-3, and caspase-1, is unchanged between both genotypes. **B:** Increased immunoreactivities for oxidative stress markers, COX, Mn-SOD, and AIF, are observed in the inner segment of *Uchl3*-deficient mice (**arrows**). Translocation of Endo G to nuclei is found in the outer nuclear layer of *Uchl3*-deficient mice (**inset** in **B**). OS, outer segment; IS, inner segment; ONL, outer nuclear layer; OPL, outer plexiform layer; INL, inner nuclear layer; IPL, inner plexiform layer; GCL, ganglion cell layer. Scale bars = 50 μm (**A** and **B**); 10 μm (**inset** in **B**).

mice.[29] Therefore, loss of UCH-L3 may mildly promote the cell death of these cells.

After 3w of age, prominent and progressive photoreceptor cell apoptosis was disclosed in the outer nuclear layer of *Uchl3*-deficient mice. Under pathological conditions, several apoptotic pathways have been suggested in experimental retinal degeneration. Caspase-1 is predominantly associated with photoreceptor cell apoptosis in retinal degeneration of ischemia-reperfusion.[30] Light-induced retinal degeneration activates the parallel cascades, caspase-1[20] and caspase-independent apoptosis.[21] Oxidative stress leads to caspase-independent apoptosis in cultured cells.[31] Our results indicated that a caspase-independent pathway was activated during photoreceptor cell apoptosis in *Uchl3*-deficient mice, because immunohistochemical analysis revealed that activated caspase-3 and caspase-1 were not expressed in the degenerated retina. In addition, Endo G, a protein involved in the caspase-independent pathway, was expressed in the nuclei of the outer nuclear layer in *Uchl3*-deficient mice. Endo G is a mitochondria-specific nuclease that translocates to nuclei and serves as the DNase during a caspase-independent apoptosis.[32] Therefore, Endo G may be responsible for the DNA degradation that occurs during apoptosis in *Uchl3*-deficient mice. Expression of Endo G was slightly increased in the outer plexiform layer, inner nuclear layer, and inner plexiform layer of the *Uchl3*-deficient mice after 3w of age despite no significant UCH-L3 immunoreactivities in these layers. This result may reflect trans-synaptic secondary neuronal degeneration or glial changes of Müller cells.

AIF, another factor involved in caspase-independent apoptosis, was enriched in the inner segment; however, we did not observe translocation to nuclei for this protein. AIF is a mitochondrial flavoprotein that is a free radical scavenger of healthy cells.[33] During apoptotic induction, AIF translocates from mitochondria to nuclei.[33,34] It functions as a caspase-independent and PARP-1-dependent death effector that induces chromatin condensation and large-scale DNA fragmentation.[35] In our study, expression of AIF at the inner segment was associated with increased immunoreactivities of the oxidative stress markers, COX and Mn-SOD. Although it is unknown why AIF did not translocate to nuclei in the degenerated retina, increased immunoreactivity for AIF in the inner segment may indicate a reaction to oxidative stress. Because mouse eyes open 12 to 13 days after birth, light-induced oxidative stress may affect photoreceptor cell apoptosis in *Uchl3*-deficient mice after development. On the other hand, the retinal oxygen consumption increases under dark-adapted condition in the cat retina.[28,36] It may be interesting to study whether constant light or constant dark has any effect on the development of retinal degeneration in the *Uchl3*-deficient mice.

Uchl3-Deficient Mice as a Model of Retinal Degeneration with Mitochondrial Impairment

Apoptosis during retinal degeneration is observed in inherited diseases such as retinitis pigmentosa as well as in retinal diseases induced by a variety of stimuli, including hypoxia and oxidative stresses.[37,38] Several genetically engineered animal models of retinitis pigmentosa have been extensively investigated, including the RCS rat and *rd* mice. Retinal degeneration in the RCS rat was originally identified as an impairment of phagocytosis by pigmented epithelium due to mutation of receptor ty-

Table 1. Chronological Changes in Expression of Markers for Oxidative Stress and Caspase-Independent Apoptosis

	COX						Mn-SOD						AIF						Endo G					
	P0	P10	3w	6w	8w	12w	P0	P10	3w	6w	8w	12w	P0	P10	3w	6w	8w	12w	P0	P10	3w	6w	8w	12w
VZ*	−						−						−						−					
PR		−						−						−						−				
OS			−	−	nd	nd			−	−	nd	nd			−	−	nd	nd			−	−	nd	nd
IS			+	+	−	nd			+	+	+	nd			++	+	−	nd			−	−	−	nd
ONL		−	−	−	−	−		−	−	−	−	−		−	−	−	−	−		−	++§	+§	−	−
OPL		−	−	−	−	−		−	−	−	−	−		−	−	−	−	−		−	±	±	±	±
INL		−	−	−	−	−		−	−	−	−	−		−	−	−	−	−		−	±§	±§	−	−
IPL	−	−	−	−	−	−	−	−	−	−	−	−	−	−	−	−	−	−	−	−	−	−	±	±
GCL	−	−	−	−	−	−	−	−	−	−	−	−	−	−	−	−	−	−	−	−	−	−	−	−

*VZ, ventricular zone; PR, photoreceptor; OS, outer segment; IS, inner segment; ONL, outer nuclear layer; OPL, outer plexiform layer; INL, inner nuclear layer; IPL, inner plexiform layer; GCL, ganglion cell layer.
−, no change; ±, slight increase; +, mild increase; and ++, marked increase of immunoreactivity compared to that of wild type.
nd, not determined due to atrophic change.
§Nuclear staining.

rosine kinase (Mertk) with subsequent photoreceptor cell death occurring in a caspase-1- and -2-dependent manner.[39–42] *rd* mice have a recessive mutation in the rod cGMP phosphodiesterase β-subunit, and photoreceptor apoptosis occurs via a caspase-dependent mechanism.[43,44] Thus, these animal models of retinitis pigmentosa differ from *Uchl3*-deficient mice with regard to the mechanism of retinal degeneration.

The relationship between retinal degeneration and mitochondrial dysfunction has not been well studied except in Harlequin mice, which contain a mutation of AIF and exhibit progressive retinal degeneration.[45] We consider that the degeneration induced in the *Uchl3*-deficient mice is associated with mitochondrial dysfunction, because mitochondria in the inner segment of mutant retina exhibited morphological changes such as decreased cristae area. *Uchl3*-deficient mice reveal not only retinal degeneration but also muscle degeneration and mild growth retardation,[17] and thus the lack of UCH-L3 may affect general organs containing abundant mitochondria. Subtypes of mitochondrial diseases, such as chronic progressive external ophthalmoplegia and Kearns-Sayre syndrome, are caused by various mitochondrial DNA deletions and observed progressive ophthalmoplegia as well as retinitis pigmentosa.[46,47] Because UCH-L3 is predicted to be involved in the maintenance of mitochondrial function, *Uchl3*-deficient mice may be a model of disease that arises from mitochondrial impairment. Further studies are necessary to clarify the molecular mechanisms underlying retinal degeneration, as well as other organs in these animals.

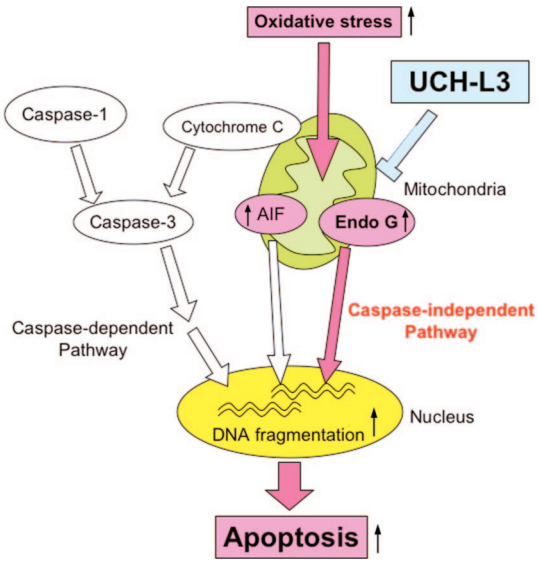

Figure 7. Function of UCH-L3 in apoptosis during retinal degeneration. Mitochondrial apoptosis is classified into caspase-dependent and caspase-independent pathways. Loss of UCH-L3 leads to oxidative stress-induced mitochondrial damage that causes translocation of Endo G from mitochondria to nuclei, resulting in caspase-independent apoptosis. **Red arrows** are considered to be activated in *Uchl3*-deficient mice.

Acknowledgments

We thank Dr. S.M. Tilghman for providing *Uchl3*-deficient mice, Dr. K. Oyanagi, Dr. T. Harada, and Dr. K. Arima for their useful discussions, Ms. H. Fujita and Mr. D. Yamada for the breeding and care of the mice, and Mr. R. Debold, Ms. T. Matsuzawa, and Mr. N. Takagaki for editing the manuscript.

References

1. Amerik AY, Hochstrasser M: Mechanism and function of deubiquitinating enzymes. Biochim Biophys Acta 2004, 1695:189–207
2. Weissman AM: Themes and variations on ubiquitylation. Nat Rev Mol Cell Biol 2001, 2:169–178
3. Pickart CM, Eddins MJ: Ubiquitin: structures, functions, mechanisms. Biochim Biophys Acta 2004, 1695:55–72
4. Aguilar RC, Wendland B: Ubiquitin: not just for proteasomes anymore. Curr Opin Cell Biol 2003, 15:184–190
5. Wilkinson KD: Regulation of ubiquitin-dependent processes by deubiquitinating enzymes. FASEB J 1997, 11:1245–1256
6. Doran JF, Jackson P, Kynoch PA, Thompson RJ: Isolation of PGP 9.5, a new human neurone-specific protein detected by high-resolution two-dimensional electrophoresis. J Neurochem 1983, 40:1542–1547
7. Wilkinson KD, Lee KM, Deshpande S, Duerksen-Hughes P, Boss JM, Pohl J: The neuron-specific protein PGP 9.5 is a ubiquitin carboxyl-terminal hydrolase. Science 1989, 246:670–673
8. Osawa Y, Wang YL, Osaka H, Aoki S, Wada K: Cloning, expression, and mapping of a mouse gene, Uchl4, highly homologous to human and mouse Uchl3. Biochem Biophys Res Commun 2001, 283:627–633

9. Liu Y, Fallon L, Lashuel HA, Liu Z, Lansbury PT Jr,: The UCH-L1 gene encodes two opposing enzymatic activities that affect alpha-synuclein degradation and Parkinson's disease susceptibility. Cell 2002, 111:209–218
10. Leroy E, Boyer R, Auburger G, Leube B, Ulm G, Mezey E, Harta G, Brownstein MJ, Jonnalagada S, Chernova T, Dehejia A, Lavedan C, Gasser T, Steinbach PJ, Wilkinson KD, Polymeropoulos MH: The ubiquitin pathway in Parkinson's disease. Nature 1998, 395:451–452
11. Saigoh K, Wang YL, Suh JG, Yamanishi T, Sakai Y, Kiyosawa H, Harada T, Ichihara N, Wakana S, Kikuchi T, Wada K: Intragenic deletion in the gene encoding ubiquitin carboxy-terminal hydrolase in *gad* mice. Nat Genet 1999, 23:47–51
12. Wilkinson KD, Deshpande S, Larsen CN: Comparisons of neuronal (PGP 9.5) and non-neuronal ubiquitin C-terminal hydrolases. Biochem Soc Trans 1992, 20:631–637
13. Kurihara LJ, Semenova E, Levorse JM, Tilghman SM: Expression and functional analysis of *Uch-L3* during mouse development. Mol Cell Biol 2000, 20:2498–2504
14. Wada H, Kito K, Caskey LS, Yeh ET, Kamitani T: Cleavage of the C-terminus of NEDD8 by UCH-L3. Biochem Biophys Res Commun 1998, 251:688–692
15. Gan-Erdene T, Nagamalleswari K, Yin L, Wu K, Pan ZQ, Wilkinson KD: Identification and characterization of DEN1, a deneddylase of the ULP family. J Biol Chem 2003, 278:28892–28900
16. Kwon J, Wang YL, Setsuie R, Sekiguchi S, Sato Y, Sakurai M, Noda M, Aoki S, Yoshikawa Y, Wada K: Two closely related ubiquitin C-terminal hydrolase isozymes function as reciprocal modulators of germ cell apoptosis in cryptorchid testis. Am J Pathol 2004, 165:1367–1374
17. Semenova E, Wang X, Jablonski MM, Levorse J, Tilghman SM: An engineered 800 kilobase deletion of *Uchl3* and *Lmo7* on mouse chromosome 14 causes defects in viability, postnatal growth and degeneration of muscle and retina. Hum Mol Genet 2003, 12:1301–1312
18. Chang GQ, Hao Y, Wong F: Apoptosis: final common pathway of photoreceptor death in rd, rds, and rhodopsin mutant mice. Neuron 1993, 11:595–605
19. Cook B, Lewis GP, Fisher SK, Adler R: Apoptotic photoreceptor degeneration in experimental retinal detachment. Invest Ophthalmol Vis Sci 1995, 36:990–996
20. Grimm C, Wenzel A, Hafezi F, Remè CE: Gene expression in the mouse retina: the effect of damaging light. Mol Vis 2000, 6:252–260
21. Donovan M, Cotter TG: Caspase-independent photoreceptor apoptosis in vivo and differential expression of apoptotic protease activating factor-1 and caspase-3 during retinal development. Cell Death Differ 2002, 9:1220–1231
22. Osborne NN, Melena J, Chidlow G, Wood JP: A hypothesis to explain ganglion cell death caused by vascular insults at the optic nerve head: possible implication for the treatment of glaucoma. Br J Ophthalmol 2001, 85:1252–1259
23. Adler R, Curcio C, Hicks D, Price D, Wong F: Cell death in age-related macular degeneration. Mol Vis 1999, 5:31
24. Harada T, Harada C, Wang YL, Osaka H, Amanai K, Tanaka K, Takizawa S, Setsuie R, Sakurai M, Sato Y, Noda M, Wada K: Role of ubiquitin carboxy terminal hydrolase-L1 in neural cell apoptosis induced by ischemic retinal injury in vivo. Am J Pathol 2004, 164:59–64
25. Kwon J, Wang YL, Setsuie R, Sekiguchi S, Sakurai M, Sato Y, Lee WW, Ishii Y, Kyuwa S, Noda M, Wada K, Yoshikawa Y: Developmental regulation of ubiquitin C-terminal hydrolase isozyme expression during spermatogenesis in mice. Biol Reprod 2004, 71:515–521
26. Osaka H, Wang YL, Takada K, Takizawa S, Setsuie R, Li H, Sato Y, Nishikawa K, Sun YJ, Sakurai M, Harada T, Hara Y, Kimura I, Chiba S, Namikawa K, Kiyama H, Noda M, Aoki S, Wada K: Ubiquitin carboxy-terminal hydrolase L1 binds to and stabilizes monoubiquitin in neuron. Hum Mol Genet 2003, 12:1945–1958
27. De Robertis E: Electron microscope observations on the submicroscopic organization of the retinal rods. J Biophys Biochem Cytol 1956, 2:319–330
28. Linsenmeier RA, Braun RD: Oxygen distribution and consumption in the cat retina during normoxia and hypoxemia. J Gen Physiol 1992, 99:177–197
29. Young RW: Cell death during differentiation of the retina in the mouse. J Comp Neurol 1984, 229:362–373
30. Katai N, Yoshimura N: Apoptotic retinal neuronal death by ischemia-reperfusion is executed by two distinct caspase family proteases. Invest Ophthalmol Vis Sci 1999, 40:2697–2705
31. Carmody RJ, Cotter TG: Oxidative stress induces caspase-independent retinal apoptosis in vitro. Cell Death Differ 2000, 7:282–291
32. Li LY, Luo X, Wang X: Endonuclease G is an apoptotic DNase when released from mitochondria. Nature 2001, 412:95–99
33. Susin SA, Lorenzo HK, Zamzami N, Marzo I, Snow BE, Brothers GM, Mangion J, Jacotot E, Costantini P, Loeffler M, Larochette N, Goodlett DR, Aebersold R, Siderovski DP, Penninger JM, Kroemer G: Molecular characterization of mitochondrial apoptosis-inducing factor. Nature 1999, 397:441–446
34. Lorenzo HK, Susin SA, Penninger J, Kroemer G: Apoptosis inducing factor (AIF): a phylogenetically old, caspase-independent effector of cell death. Cell Death Differ 1999, 6:516–524
35. Yu SW, Wang H, Poitras MF, Coombs C, Bowers WJ, Federoff HJ, Poirier GG, Dawson TM, Dawson VL: Mediation of poly(ADP-ribose) polymerase-1-dependent cell death by apoptosis-inducing factor. Science 2002, 297:259–263
36. Linsenmeier RA: Effects of light and darkness on oxygen distribution and consumption in the cat retina. J Gen Physiol 1986, 88:521–542
37. Pacione LR, Szego MJ, Ikeda S, Nishina PM, McInnes RR: Progress toward understanding the genetic and biochemical mechanisms of inherited photoreceptor degenerations. Annu Rev Neurosci 2003, 26:657–700
38. Phelan JK, Bok D: A brief review of retinitis pigmentosa and the identified retinitis pigmentosa genes. Mol Vis 2000, 6:116–124
39. D'Cruz PM, Yasumura D, Weir J, Matthes MT, Abderrahim H, LaVail MM, Vollrath D: Mutation of the receptor tyrosine kinase gene Mertk in the retinal dystrophic RCS rat. Hum Mol Genet 2000, 9:645–651
40. Feng W, Yasumura D, Matthes MT, LaVail MM, Vollrath D: Mertk triggers uptake of photoreceptor outer segments during phagocytosis by cultured retinal pigment epithelial cells. J Biol Chem 2002, 277:17016–17022
41. Katai N, Kikuchi T, Shibuki H, Kuroiwa S, Arai J, Kurokawa T, Yoshimura N: Caspase-like proteases activated in apoptotic photoreceptors of Royal College of Surgeons rats. Invest Ophthalmol Vis Sci 1999, 40:1802–1807
42. Vollrath D, Feng W, Duncan JL, Yasumura D, D'Cruz PM, Chappelow A, Matthes MT, Kay MA, LaVail MM: Correction of the retinal dystrophy phenotype of the RCS rat by viral gene transfer of Mertk. Proc Natl Acad Sci USA 2001, 98:12584–12589
43. Jomary C, Neal MJ, Jones SE: Characterization of cell death pathways in murine retinal neurodegeneration implicates cytochrome c release, caspase activation, and bid cleavage. Mol Cell Neurosci 2001, 18:335–346
44. Lem J, Flannery JG, Li T, Applebury ML, Farber DB, Simon MI: Retinal degeneration is rescued in transgenic rd mice by expression of the cGMP phosphodiesterase β subunit. Proc Natl Acad Sci USA 1992, 89:4422–4426
45. Klein JA, Longo-Guess CM, Rossmann MP, Seburn KL, Hurd RE, Frankel WN, Bronson RT, Ackerman SL: The harlequin mouse mutation downregulates apoptosis-inducing factor. Nature 2002, 419:367–374
46. Land JM, Morgan-Hughes JA, Hargreaves I, Heales SJ: Mitochondrial disease: a historical, biochemical, and London perspective. Neurochem Res 2004, 29:483–491
47. Schmiedel J, Jackson S, Schäfer J, Reichmann H: Mitochondrial cytopathies. J Neurol 2003, 250:267–277